

A New Model to Predict the Unsteady Production of Fractured Horizontal Wells (Model Baharu untuk Meramalkan Pengeluaran tak Menentu Telaga Mendatar yang Retak)

FANHUI-ZENG*, XIAOZHAO-CHENG, JIANCHUN-GUO, CHUAN LONG & YUBIAO-KE

ABSTRACT

Based on the hydraulic fracture width gradually narrows along the fracture length, with consideration of the mutual influences of fracture, non-uniform inflow of fractures segments and variable mass flow in the fracture comprehensively, a spatial separation method and time separation method were used to establish fracture horizontal well's dynamic coupling model of reservoir seepage and fracture flow. The results showed that the calculation productivity of variable width model is higher than that of the fixed width model, while the difference becomes smaller as time increase. Due to mutual interference of the fractures, the production of outer fracture is higher than that of the inner fracture. When the dimensionless fracture conductivity is 0.1, the middle segment of the fracture dominates the productivity and local peak emerges near the horizontal well. The flow in the fracture is with the 'double U' type distribution. As the dimensionless fracture conductivity increase, the fractures productivity mainly through the tips and the flow in the fractures with the 'U' type distribution. Using the established fracture width variable productivity prediction model, one can achieve the quantitative optimization of fracture shape.

Keywords: Fractured horizontal well; fracture shape quantitative optimization; flux; unsteady productivity; variable fracture width

ABSTRAK

Berdasarkan lebar retak hidraulik beransur-ansur sempit sepanjang kepanjangan retak, dengan pertimbangan retak pengaruh bersalingan, aliran masuk segmen retak tak seragam dan pemboleh ubah aliran jisim dalam retak secara menyeluruh, kaedah pemisahan ruwang dan masa telah digunakan untuk menubuhkan model gandingan dinamik telaga melintang retak aliran takungan tirsan dan retak. Keputusan kajian menunjukkan bahawa produktiviti pengiraan model kelebaran berubah-ubah adalah lebih tinggi daripada model dengan kelebaran tetap, namun perbezaan menjadi lebih kecil dengan peningkatan masa. Disebabkan keretakan gangguan itu bersalingan, penghasilan retak bahagian luar adalah lebih tinggi daripada retak dalaman. Apabila konduktiviti retak tanpa dimensi adalah 0.1, segmen tengah retak menguasai produktiviti dan puncak tempatan muncul berhampiran telaga mendatar. Aliran dalam retakan adalah dengan taburan jenis 'dua U'. Semasa konduktiviti retak tanpa dimensi meningkat, produktiviti retak terutamanya menerusi aliran hujung dan dalam retak bersama dengan taburan jenis 'U'. Dengan menggunakan model peramalan produktiviti retak lebar pemboleh ubah yang ditubuhkan, pengoptimuman kuantitatif bentuk retak boleh dicapai.

Kata kunci: Kelebaran retak pemboleh ubah; pengoptimuman kuantitatif bentuk retak; produktiviti tak menentu; taburan fluks; telaga mendatar yang retak

INTRODUCTION

Horizontal well hydraulic with multi-fractures has been proven to be one of the key technologies for successful development of tight formations, several analytical models have been proposed by different investigators for rate forecasting of horizontal wells with multi-stage hydraulic fractures (Li et al. 2013; Xiao et al. 2009; Yuan et al. 2009). Giger et al. (1984) presented the first mathematical model for analyzing productivity of horizontal wells intersecting fractures, in which flow in the rock matrix and fractures were formulated for the short and long horizontal wells and then combined to obtain a radial flow equation for the whole flow path from external boundary to wellbore. Gringarten and Raghavan (1975) considering the infinite conductivity and uniform flux fractures intercepted by a

vertical wellbore, used the Green function for the transient flow of a slightly compressible fluid in a homogeneous and anisotropic porous medium, while the infinite conductivity assumption only valid for highly conductive fractures (Joshi et al. 1987). Mukherjee and Economides (1991) developed a simplified steady state approach to calculate the number of infinite conductivity fractures with the correlation for dimensionless wellbore radius derived by Joshi et al. (1988) and Prats (1961). Raghavan et al. (1993) used the effective wellbore radius concept represent of the fractures, presenting a steady flow solution based on uniform flux along the fracture length to calculate the productivity of a horizontal well with multiple transverse hydraulic fractures under steady state conditions. Wei et al. (2005) treated the artificial fractures as fractures skin,

suggesting an analytical model for pseudo steady state productivity index of a horizontal well with multiple transverse hydraulic fractures. Guo and Schechter (1999) had pointed out that the previous inflow performance relationship equations are not accurate due to the unrealistic assumptions used, such as infinite conductivity or treat the fractures as skin. They proposed a more rigorous mathematical model for predicting performance of horizontal wells intersecting fractures fully penetrating reservoir sections. The unique feature of these new models is that flow in the fractures is taken into account and the circular geometry of the fracture imposes radial flow within the fracture of uniform flux, which one step is closer to the reality in the fractured reservoirs.

In general, different fracture geometries assumption may lead to different fracture flow rate. If the fracture is a long rectangle instead of radial flow, would result in linear flow dominates in the fracture. Because the estimation of rate is strongly affected by specific characteristics of certain fracture conductivity and half length, production model should take into account the correct fracture geometry. Cinco and Samaniego (1981) used Green's and source functions semi-analytical general solutions for the transient behavior of a vertical well intersected by a finite vertical fracture in an infinite slab reservoir. The fracture is represented by a rectangular parallelepiped porous medium of dimensions with constant fracture width along the fracture. Larsen et al. (1994, 1991) established a model of fractured horizontal well at an unsteady state based on numerical integration of Laplace transformed point-source solutions for unbounded reservoirs in three dimensions. Laplace transformed solutions for uniform flux fractures in unbounded 3D reservoirs are first developed. From the uniform flux cases, solutions for flow to finite conductivity fractures intercepted by a horizontal wellbore are developed by the approach used by Cinco and Samaniego (1981) build solutions from uniform flux segments with unknown rates and then determined rates as solutions of a linear system of equations defined from continuity in pressure and flux from the formation to the fracture and between segments within the fracture. Raghavan et al. (1997) used vertical well fracture models (Cinco et al. 1978) proposed these models assume uniform flux or infinite conductivity rectangular fractures and the fracture communicates with the wellbore over its entire height to approximate the pressure transient responses of fractured horizontal wells. Al Kobaisi et al. (2006) presents a hybrid numerical-analytical model for the pressure transient performance of fractured horizontal wells and the fracture is represented by a rectangular parallelepiped porous medium. Wang et al. (2009) based on the uniform flux pseudo-steady state equivalent wellbore radius model, variable mass linear flow model of constant fractures to develop a model for predicting the productivity of hydraulic horizontal wells.

All the above approach have investigated the theoretical models based on the reservoir seepage coupling with artificial fracture flow, but the theory

of the fluid flow inside the fracture description is not comprehensive, which are deduced assumed the flux along with the fracture to be uniform or non-uniform flow and constant width along the fracture. In fact, the fracture width may be variable because of an elliptical cross-section (van Eekelen 1982), and conductivity also can be variable within the fracture because of non-uniform gel and prop pant placement or non-planar fracture profile. Soliman et al. (1978) showed that the distribution and magnitude of the conductivity within the fracture had a significant influence on the performance of the fracture and the use of average fracture conductivity was not appropriate in these cases. In this study, the general solution for the rate calculation of a horizontal well intersected by finite conductivity vertical fractures was presented. Based on non-steady flow theory, potential principles, superposition principle and time superposition principle, a new method of predicting the productivity of fractured horizontal wells with the consideration of the non-uniform flux distribution and variable width along the fracture is presented, which makes the results more reasonable. The factors influencing the productivity and field application are presented in this article as well.

MATHEMATICAL MODEL

ASSUMPTIONS

In order to set up the mathematical model, some assumptions are done as follows (Sun et al. 2012; Wang et al. 2009):

The oil reservoir is closed at top and bottom. The infinite isotropic reservoir has a constant height h , porosity ϕ and permeability K . At the initial time $t = 0^+$, the pressure is uniform throughout the oil reservoir and is equal to p_i ; The fractured horizontal well locates in the center of oil reservoir (Figure 1). The well is parallel to y -axis with the length L , the number of fractures is N . The fractures are vertical to wellbore and equal or unequal space from each other, the length of the k th fractures x_{fk} are equal or unequal with each other, which fully penetrate the reservoir. The length is x_{fk} height is h and width is w_{fk} , in x , z and y directions and the heel width is $w_{fk,max}$ and the toe width is $w_{fk,min}$; Single-phased and slightly compressible fluid flows in reservoir. Compressibility coefficient c_t and viscosity μ is constant. Ignore pressure drop of the fluid flow in the horizontal wellbore.

RESERVOIR SEEPAGE MODEL

With consideration of the fractures fully penetrate the reservoir and the magnitude of fractures is smaller than that of reservoir, the hydraulic horizontal well fractures flow system can be simplified as a radial flow within infinite plane reservoir (Zeng et al. 2008). For convenience, the both monoplanes of the fracture are divided into ns equal segments and with a length of $\Delta x_{fk} = x_{fk}/ns$ and also there are ns reservoir nodes lie closest to the fracture nodes in

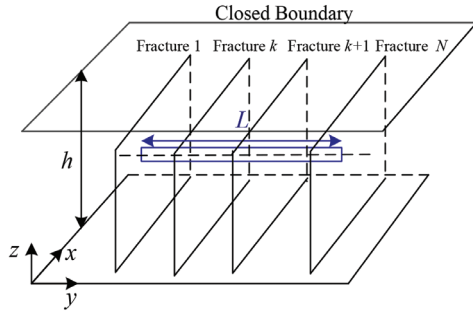


FIGURE 1. The physical model of fractured horizontal well in an infinite reservoir

the reservoir and each reservoir node is considered as one sink point as shown in Figure 2.

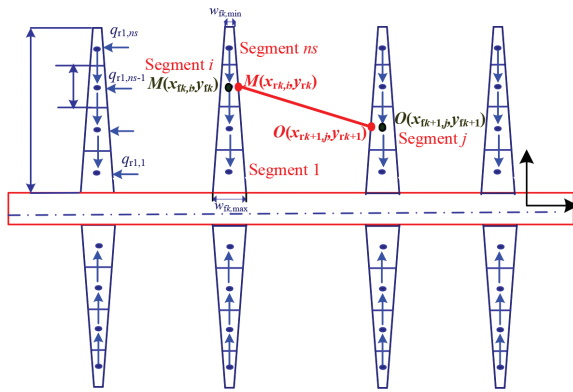


FIGURE 2. The sectional schematic of the fracture and reservoir node in the model

The reservoir pressure rearranges because of the appearance of the artificial fractures. The output of the sink points keeps declining over the production duration. However, if the time interval section is taken as small as possible, the output can be treated as constant rate. Under the Cartesian Coordinates Plane, based on the pressure drawdown equation of the flow with constant rate in an infinite isotropic reservoir, the pressure drawdown of the reservoir point $O(x_{rk+1,j}, y_{rk+1})$ caused by the reservoir sink point $M(x_{rk,i}, y_{rk})$ at time t as follow.

$$\begin{aligned} \Delta p_{rk+1,j}(t) &= p_i - p_{rk+1,j}(t) \\ &= \frac{q_{rk,i} \mu B}{4\pi K h} \left\{ -Ei \left(\frac{(x_{rk,i} - x_{rk+1,j})^2 + (y_{rk,i})^2}{4\eta t} \right) \right\}, \quad (1) \end{aligned}$$

where, $q_{rk,i}$ is a source term representing the flux entering the fracture from the reservoir at a point $M(x_{rk,i}, y_{rk})$ closed to the fracture surface.

where $\Delta p_{rk+1,j}(t)$ gives the pressure drop at the reservoir node $O(x_{rk+1,j}, y_{rk+1})$ due to the flow from the reservoir node $M(x_{rk,i}, y_{rk})$; p_i is the initial pressure of the reservoir, MPa;

$p_{rk+1,j}(t)$ is the pressure of reservoir node $M(x_{rk,i}, y_{rk})$ at time t , MPa; $q_{rk,i}$ is the flow rate that from the reservoir node $M(x_{rk,i}, y_{rk})$ to the fracture node $M(x_{rk,i}, y_{rk})$; B is the fluid volume factor, dimensionless; $(x_{rk,i}, y_{rk})$ are the coordinates of reservoir node M ; $(x_{rk+1,j}, y_{rk+1})$ are the coordinates of reservoir node O ; K is the reservoir permeability, D; h is the reservoir thickness, m; η is transmissibility to diffusivity, m^2/ks ; $\eta = K/(\mu c \phi)$; μ is the fluid viscosity, mPa·s; c is the total compressibility, MPa^{-1} ; ϕ is the porosity, decimal number; and t is the production duration time, ks.

Equation (1) can be applied for each reservoir node. The interaction between nodes can be taken into account by superposition of pressures in space. For example, when there are $N \times 2ns$ nodes in the reservoir, the total pressure drops at the point $O(x_{rk+1,j}, y_{rk+1})$ of the production time t can be taken into account by the superposition principle of the potential in space:

$$\begin{aligned} \Delta p_{rk+1,j}(t) &= p_i - p_{rk+1,j}(t) = \sum_{k=1}^N \sum_{i=1}^{2ns} \frac{q_{rk,i} \mu B}{4\pi K h} \\ &\quad \left\{ -Ei \left(\frac{(x_{rk,i} - x_{rk+1,j})^2 + (y_{rk,i} - y_{rk+1})^2}{4\eta t} \right) \right\} \\ &= \sum_{k=1}^N \sum_{i=1}^{2ns} q_{rk,i} \cdot F_{ki,k+1,j}(t), \quad (2) \end{aligned}$$

where $\Delta p_{rk+1,j}(t)$ gives the pressure drop at the reservoir node $O(x_{rk+1,j}, y_{rk+1})$ due to the flow from itself and all other reservoir nodes; N is the number of the fractures, dimensionless; ns is the equal segments of monoplanes;

$$F_{ki,k+1,j}(t) = \frac{\mu B}{4\pi K h} \left\{ -Ei \left(\frac{(x_{rk,i} - x_{rk+1,j})^2 + (y_{rk,i} - y_{rk+1})^2}{4\eta t} \right) \right\},$$

the term $F_{ki,k+1,j}(t)$ stands for the effect of reservoir node $M(x_{rk,i}, y_{rk})$ on reservoir node $O(x_{rk+1,j}, y_{rk+1})$, where $O(x_{rk+1,j}, y_{rk+1})$ is the node under consideration.

In order to calculate the unsteady reservoir seepage with (1), the principle of superposition in time is used to accomplish this task in a special way. Take the pressure dropdown calculation of reservoir node $O(x_{rk+1,j}, y_{rk+1})$ for example, at the time Δt one can write:

$$\begin{aligned} \Delta p_{rk+1,j}(\Delta t) &= p_i - p_{rk+1,j}(\Delta t) \\ &= q_{r1,1}(\Delta t) F_{11,k+1,j}(\Delta t) \\ &\quad + q_{r1,2} F_{12,k+1,j}(\Delta t) \\ &\quad + \dots + q_{rN,2ns} F_{N2ns,k+1,j}(\Delta t). \quad (3) \end{aligned}$$

The equations that result from superposition in space and time of all reservoir nodes are referred to as follows. For time = $n\Delta t$, this is the n th time step (Sun et al. 2013).

$$\begin{aligned}
 \Delta p_{rk+1,j}(n\Delta t) &= p_i - p_{rk+1,j}(n\Delta t) \\
 &= \{q_{rl,1}(\Delta t) F_{11,k+lj}(n\Delta t) + [q_{rl,1}(2\Delta t) \\
 &\quad - q_{rl,1}(\Delta t)] F_{11,k+lj}((n-1)\Delta t) \\
 &\quad + [q_{rl,1}(3\Delta t) - q_{rl,1}(2\Delta t)] F_{11,k+lj}((n-2)\Delta t) + \dots \\
 &\quad + [q_{rl,1}(n\Delta t) - q_{rl,1}((n-1)\Delta t)] F_{11,k+lj}(\Delta t)\} \\
 &\quad + \{q_{rN,2ns}(\Delta t) F_{N2ns,k+lj}(n\Delta t) + [q_{rN,2ns}(2\Delta t) \\
 &\quad - q_{rN,2ns}(\Delta t)] F_{N2ns,k+lj}((n-1)\Delta t) + [q_{rN,2ns}(3\Delta t) \\
 &\quad - q_{rN,2ns}(2\Delta t)] F_{N2ns,k+lj}((n-2)\Delta t) + \dots \\
 &\quad + [q_{rN,2ns}(n\Delta t) - q_{rN,2ns}((n-1)\Delta t)] F_{N2ns,k+lj}(\Delta t)\} \\
 &= \sum_{k=1}^N \sum_{l=1}^{2ns} \{q_{rk,i}(\Delta t) F_{ki,k+lj}(n\Delta t) + \sum_{g=2}^n [q_{rk,i}(g\Delta t) \\
 &\quad - q_{rk,i}((g-1)\Delta t)] F_{ki,k+lj}[(n-g+1)\Delta t]\}. \tag{4}
 \end{aligned}$$

Similar equations can be written for all reservoir nodes. The F 's in the above equation are defined by (2).

VARIABLE WIDTH FRACTURE FINITE-CONDUCTIVITY FLOW MODEL

This section develops a semi analytical solution for a fractured horizontal well with variable width finite conductive fractures. Take the single wing of $k+1$ th fracture for example, the fracture is divided into ns segments as shown in Figure 3. Segment 1 represents the heel of the fracture, segment ns represents the toe.

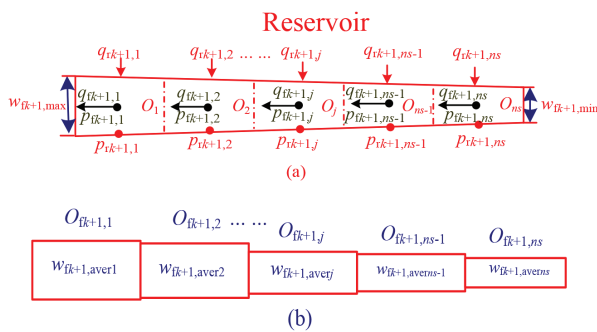


FIGURE 3. Monoplane of the fracture divided into ns segments

For each segment, the uniform flux solution of (4) is used to describe the flow rate from reservoir nodes into fracture nodes. Flow in the fracture is modeled using a fracture linear flow model that considers variable mass flow and frictional effects in the fracture. These two flows

are then coupled using the equations given below. For this problem, there are $4ns$ of unknowns in the problem, as:

- Pressures at reservoir nodes: $p_{rk+1,1}, p_{rk+1,2}, \dots, p_{rk+1,j}, \dots, p_{rk+1,ns}$;
- Pressures at fracture nodes: $p_{rk+1,1}, p_{rk+1,2}, \dots, p_{rk+1,j}, \dots, p_{rk+1,ns}$;
- Flow rates from reservoir nodes to fracture nodes: $q_{rk+1,1}, q_{rk+1,2}, \dots, q_{rk+1,j}, \dots, q_{rk+1,ns}$;
- and Flow rates in fracture segments: $q_{rk+1,1}, q_{rk+1,2}, \dots, q_{rk+1,j}, \dots, q_{rk+1,ns}$.

MASS BALANCE

Flow rate at any node in the fracture can be related by a mass balance to flow rate from the reservoir. Assuming fluid density is constant in the fracture, one can write:

$$q_{rk+1,n} = \sum_{i=n}^{ns} q_{rk+1,i} \tag{5}$$

There are ns numbers of such mass balance equations on the fracture nodes.

PRESSURE CONTINUITY

Reservoir nodal pressure is located on the outer side of the fracture at a distance w_{rk+1} from the center of the fracture, fracture nodal pressure for the same segment is located at the center of the fracture. Since the momentum equations in the fracture are one dimensional in nature, fracture nodal pressure represents the segment pressure for the entire fracture cross-section. Hence, reservoir nodal pressure can be equated to the fracture nodal pressure to establish pressure continuity between the reservoir and the fracture:

$$P_{rk+1,j} = P_{rk+1,j'} \tag{6}$$

Again a total of ns number of such equations can be written.

RESERVOIR FLOW EQUATIONS

The equations that result from superposition in space of all reservoir nodes are referred to (4). Similar ns equations can be written for the reservoir nodes.

VARIABLE WIDTH FRACTURE PRESSURE DROP EQUATIONS

The pressure at a given fracture node is related to the pressure at the downstream fracture node through the fracture momentum balance equations described next. Flow in each fracture segment is calculated using planar Darcy flow models. After that, considering the width increase gradually closer to the heel of the fracture and process the fracture profile into trapezoidal cross-section. For convenience, treat the segment as a rectangular and

take the center width as the segment width, Figure 3(b). The width of j th segment in the $k+1$ th fracture at the point $x_{fk+1,j}$ is,

$$w_{fk+1,j} = w_{fk+1,\min} + (w_{fk+1,\max} - w_{fk+1,\min}) \times \frac{(x_{fk+1} - x_{fk+1,j})}{x_{fk+1}} \quad (7)$$

and the average widths of j th the segment as follow,

$$w_{fk+1,averj} = (w_{fk+1,j} + w_{fk+1,j-1})/2, \quad (8)$$

where $w_{fk+1,j}$ is the width of the j th segment in the $k+1$ th fracture, m; $w_{fk+1,\max}$ is the heel width of the $k+1$ th fracture, m; $w_{fk+1,\min}$ is the toe width of the $k+1$ th fracture, m; $w_{fk+1,j}$ is the distance of the j th segment in the $k+1$ th fracture to the wellbore, m; and $w_{fk+1,averj}$ is the average width of j th segment in the $k+1$ th fracture, m.

Take the pressure drop calculation of the j th segment (point $O_{fk+1,j}$) in the $k+1$ th fracture to the wellbore (point $O_{fk+1,0}$) for example, frictional pressure drop is calculated using (9).

$$\begin{aligned} \Delta p_{fk+1,j-0} &= p_{fk+1,j} - p_{fk+1,0} \\ &= \frac{\mu B}{k_{fk+1} D} \frac{\Delta x_{fk+1,j}}{w_{fk+1,aver1}} q_{fk+1,1} \\ &\quad + \frac{\mu B}{k_{fk+1} D} \left(\frac{\Delta x_{fk+1,1}}{w_{fk+1,aver1}} + \frac{\Delta x_{fk+1,2}}{w_{fk+1,aver2}} \right) q_{fk+1,2} + \dots \\ &\quad + \frac{\mu B}{k_{fk+1} D} \left(\frac{\Delta x_{fk+1,1}}{w_{fk+1,aver1}} + \frac{\Delta x_{fk+1,2}}{w_{fk+1,aver2}} + \dots + \frac{\Delta x_{fk+1,j}}{w_{fk+1,averj}} \right) q_{fk+1,j} \\ &\quad + \frac{\mu B}{k_{fk+1} D} \left(\frac{\Delta x_{fk+1,1}}{w_{fk+1,aver1}} + \frac{\Delta x_{fk+1,2}}{w_{fk+1,aver2}} + \dots + \frac{\Delta x_{fk+1,j}}{w_{fk+1,averj}} \right) q_{fk+1,j+1} + \dots \\ &\quad + \frac{\mu B}{k_{fk+1} D} \left(\frac{\Delta x_{fk+1,1}}{w_{fk+1,aver1}} + \frac{\Delta x_{fk+1,2}}{w_{fk+1,aver2}} + \dots + \frac{\Delta x_{fk+1,j}}{w_{fk+1,averj}} \right) q_{fk+1,ns} \\ &= \frac{\mu B}{k_{fk+1} D} \left[\sum_{i=1}^j \left(q_{fk+1,i} \sum_{j=1}^i \frac{\Delta x_{fk+1,j}}{w_{fk+1,averj}} \right) + \sum_{n=j+1}^{ns} \left[q_{fk+1,n} \left(\sum_{i=1}^j \frac{\Delta x_{fk+1,i}}{w_{fk+1,averi}} \right) \right] \right] \quad (9) \end{aligned}$$

where K_{fk+1} is the permeability of the $k+1$ th fracture, D; w_{fk+1} is the width of the $k+1$ th fracture, m; and $\Delta x_{fk+1,j}$ is the length of each segment in the $k+1$ th fracture, m.

CONSTRAINT EQUATIONS

Since it has been assumed that the horizontal well bore is infinite conductive, there's the same pressure in anywhere of the well bore at the same time. In order to keep the pressure continuity in the fracture and well bore, (10) is established:

$$p_{fk+1,0} = p_{wf}, \quad (10)$$

where p_{wf} is the flow pressure of the well bottom, MPa.

There is no fluid flowing from other part of the well bore except the fracture section, so the total production of the fractured horizontal well can be calculated as:

$$Q = \sum_{k=1}^N \sum_{i=1}^{2ns} q_{rk,i} \quad (11)$$

Superposition in time allows us to employ any one of the above constraints during the entire time of flow. Provision is also made to start the model with the BHP constraint.

MODEL SOLUTION PROCEDURE

The number of equations for single wing of the $k+1$ th fracture that can be formed is equal to $4ns$, the same as the number of unknowns. Pressure continuity equations indicate that reservoir nodal pressures can be used instead of fracture nodal pressures. Furthermore, the mass balance equations indicate that fracture node flow rates ($q_{fk,i}$) can be replaced by reservoir node flow rates ($q_{rk,i}$) using (5). Pressures and flow rates corresponding to fracture segments can be eliminated using the pressure continuity and mass balance equations so that only the reservoir pressures and flow rates are left as unknown variables. After this reduction, there is only $2ns$ number of unknowns corresponding to the reservoir pressures ($p_{rk+1,1}, p_{rk+1,2}, \dots, p_{rk+1,j}, \dots, p_{rk+1,ns}$) and reservoir node flow rates ($q_{rk+1,1}, q_{rk+1,2}, \dots, q_{rk+1,j}, \dots, q_{rk+1,ns}$). These unknowns can be calculated from the $2ns$ number of equations given by (4) and (9). It should be noted that the flow bottom pressure of the first fracture segment calculated by (10) and the average width of the segment calculated by (7) and (8) is part of (9). This reduction in variables reduces the computational time needed to solve the equations implicitly by Iterative method.

RESULTS AND DISCUSSION

A computer program is designed to test this model and compare with uniform flux with radial flow in the fracture and infinite-conductivity of the fractured horizontal well mode, the basic parameter values of this case study are shown in Table 1. The number of fractures is limited to a maximum of four in this study. For the sake of simplicity, we assume that the fractures are of equal size and are equally spaced in the reservoir.

MODEL VALIDATION

The case study was run with the well bottom flow pressure constraint of 25 MPa. Table 2 presents the fracture and daily production comparison with different models and the actual production.

The result showed that the computational results with the proposed model which with non-uniform flux and finite conductivity is closer to the actual productivity. While the Eclipse simulation results, i.e. Infinite conductivity model calculates the 1st day production of 62.025 m³/d that far exceeded the actual value, which indicates that the impact of pressure loss within the fracture cannot be

TABLE 1. Basic parameters of a real example

Parameters	Data	Parameters	Data
Horizontal well length, L_f	400 m	Oil Density at Reservoir Conditions, ρ	870 kg/m ³
Reservoir Height, h	12 m	Bottom flow pressure, p_{wf}	25 MPa
Permeability, K	0.0035 D	Well Diameter, r_w	0.0889 m
Porosity, ϕ	10 %	Fracture permeability, K_f	30 D
Total Compressibility, c_t	0.00035 MPa ⁻¹	Fracture heel width, w_{kmax}	5.0 mm
Reservoir Initial pressure, p_i	30 MPa	Fracture toe width, w_{kmin}	0.5 mm
Formation Volume Factor, B	1.084	Fracture length, x_{fk}	75 m
Oil Viscosity, μ	8 mPa·s	Fracture numbers, N	4

TABLE 2. Comparison of simulated solution and the actual productivity

Parameters	Productivity (m ³ /d)											
	Presented model $w_{max}=5.00mm, w_{min}=0.50mm$			Kobaisi's model(2006) $w_{aver}=2.75mm$			Eclipse simulation results Infinite conductivity			Actual production		
	1 d	10 d	120 d	1 d	10 d	120 d	1 d	10 d	120 d	1 d	10 d	120 d
Fracture 1	5.992	3.318	1.743	5.513	3.157	1.689	15.731	5.814	2.495	/	/	/
Fracture 2	5.901	2.659	1.209	5.435	2.567	1.200	15.281	3.855	1.223	/	/	/
Fracture 3	5.901	2.659	1.209	5.435	2.567	1.200	15.281	3.855	1.223	/	/	/
Fracture 4	5.992	3.318	1.743	5.513	3.157	1.689	15.731	5.814	2.495	/	/	/
Total production	23.786	11.955	5.905	21.896	11.449	5.778	62.025	19.339	7.435	23.220	11.549	5.750

omitted. The results also showed that the constant width case has less productivity than the variable width case. The reason for this is that as more and more oil flow close to the heel of the fracture, which will produce an extra resistance, while increase the fracture width will promote the productivity increase and gain access to the well bore more easily.

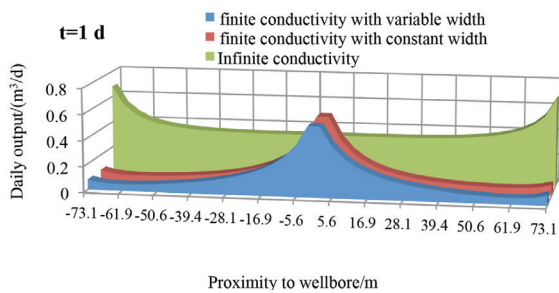


FIGURE 4. Production distribution of fractures with different models

Figure 4 is the flux distribution along the discrete segments of the 1st fracture at time $t = 1$ d with different model. The infinite model did not take into consideration the pressure drop within the fracture, the flux distribution is a ‘U shape’, with the flow at the two ends being relatively high, which is consistent with the distribution pattern stated in the literature (Li et al. 2013). The proposed model

considers the finite conductivity with variable fracture width along the fracture. The distribution of flow rate is wave-like shape due to the influence of fractures segments interference with consideration. As the pressure along the fracture dropped as the distance close to the wellbore, leading to a higher output of the fracture segment that was closer to the well bore. This distribution pattern is similar that referenced in the literature (Wang et al. 2009). Compare the results of variable width model with the constant width model; the output peak of model former is higher than that of the later model.

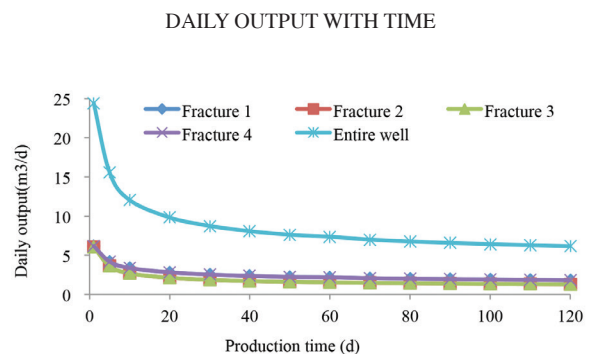


FIGURE 5. Daily production over time

Figure 5 is the daily production of hydraulic fractures and horizontal well with time. As shown as Figure 5, the daily output of fractured horizontal wells decreases rapidly

from a high value at the beginning of producing and then kept on steady at a constraint of bottom pressure. This is because when a fractured horizontal well start to produce the pressure waves has not spread to most of the flow regions at early stage, the fluid is merely flowing linearly from the bedrock around the fracture towards the fracture. When the pressure wave reach to the outer boundaries of the fractures, the flow enters the quasisteady state with the production gradually tends to be steady. Comparing with the output of fractures in different position, the flow rate is approximately equal in each fracture at the beginning and the gap between fractures is growing in the unsteady stage. The fracture output of the two ends (Fractures 1 and 4) is higher than that of the center (Fractures 2 and 3). That is the outermost fractures which have larger drainage area and the inner are existing interference between fractures. It also demonstrates that the fractures of the two ends have protective screen effect on the middle fractures and it is an effective method of increasing production to add the fracture length of the two ends.

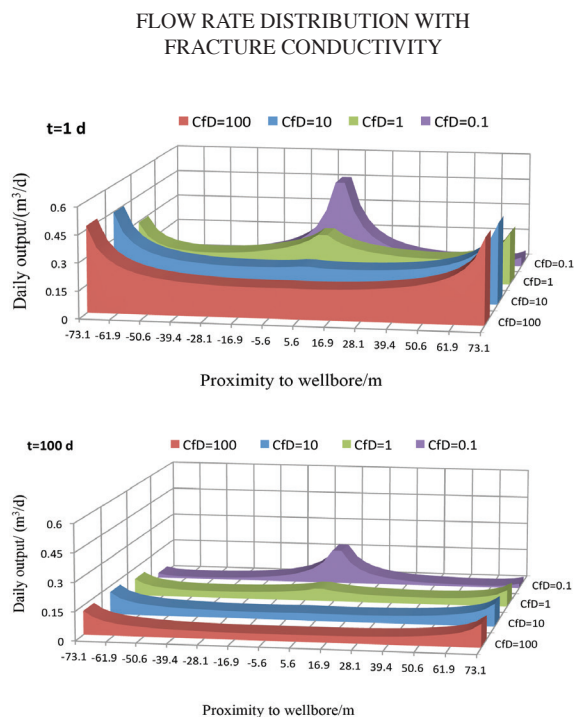


FIGURE 6. Flow distribution with fracture conductivity

Figure 6 illustrates the relationship between the flux distribution with conductivity of the 1st fracture at time t=1d and t=100d, it can be seen that the inflow of fracture segment increase as the position closer to the well bore. When the dimensionless fracture conductivity $[C_{fd}=(K_f w_{f,aver})/(Kx_p)]$ is small, the output of the center is highest with a peak and fracture conductivity is lower, the more obvious peak. As the conductivity increase, the output transfers from the center to the ends, as the fracture conductivity as large as possible and the pressure loss in the fracture can be omitted and also because of the ends of

the fracture have larger drainage area resulted in large flux, the flux distribution is a ‘U shape’. When C_{fd} is 100, the flux along the fracture exhibited a uniform characteristic, which exhibit infinite conductivity fracture characteristics.

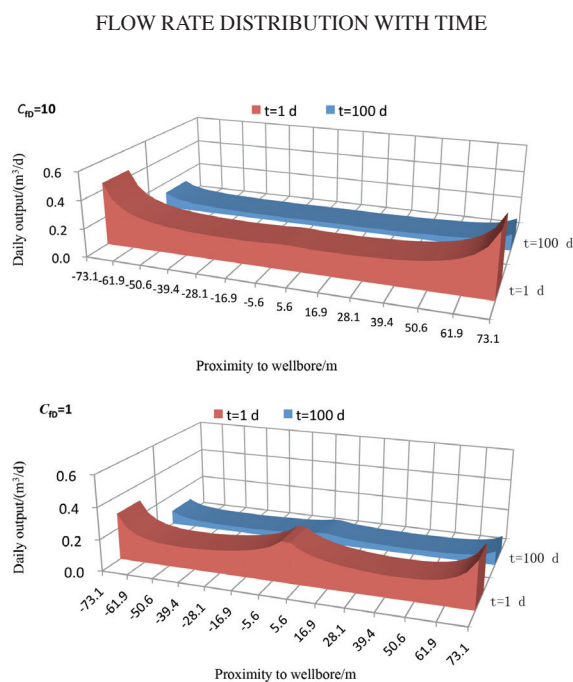


FIGURE 7. Flow rate distribution with productivity time

Figure 7 is the flow distribution of the 1st fracture at different times. At the early time, as the interference has not begun between the fractures and segments, so the output of higher conductivity ($C_{fd} \geq 10$) exhibit the feature of ‘U’ type, the yield mainly come from the ends of the fracture. The production transverse from the ends to the center with the conductivity decrease. As time increase, the reservoir pressure wave was gradually diffused outwards, which caused the flux of the center segments gradually decrease, while that at the two ends of the fracture gradually increased, the characteristic of uniform fluid production was basically exhibited along the entire fracture.

FRACTURE WIDTH PROFILE OPTIMIZATION

Figure 8 illustrates the relationship between the cumulative productions with 4 different width distribution schemes along the fracture of 360 d. Where scheme I is $w_{max}=w_{min}=2.75$ mm, scheme II is $w_{max}=3$ mm, $w_{min}=2.5$ mm, scheme III is $w_{max}=4$ mm, $w_{min}=1.5$ mm and scheme IV is $w_{max}=5$ mm and $w_{min}=0.5$ mm. It is clear that under the same average width, the gaps are great of different schemes (scheme I is 2020 m³ and scheme IV is 2319 m³) under different fracture width distribution, which implies that the productivity can be increased by the optimization of width distribution. As the effect of variable fracture width on cumulative production, the cumulative output increases rapidly as the difference of heel width and toe width, when the difference increase

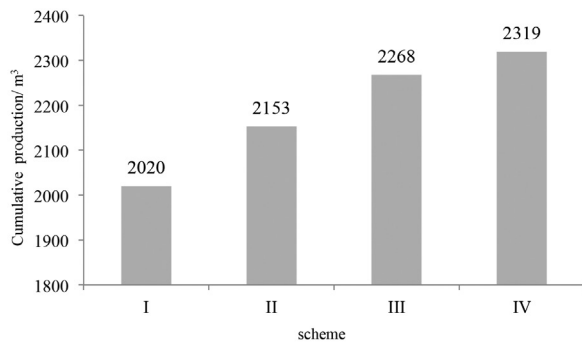


FIGURE 8. Cumulative production of different scheme

to a certain value, the change of fracture width has little influence on the productivity and there is an optimized fracture width distribution. The main reason is that when the fracture width between the heel and toe is too small and gas reservoir seepage capacity is relatively strong, the fluid near the fracture encounters extra resistance. Then by increasing the fracture conductivity eliminate this additional resistance, we can ensure that production increased significantly. When fracture width at the heel is too high, while the gas reservoir supply cannot keep up, which manifested the 'evacuation' phenomenon, performance as an increase in width difference, output growth is reduced. Therefore, there is optimized fracture width consistent with the reservoir supply capability for certain reservoir. In this example, the width at the heel is 4 mm while the toe is 1.5 mm.

CONCLUSION

A reservoir/fractured horizontal well coupling model are established for finite fracture conductivity considering the mutual interferences of fractures and segments under unsteady state. The computational solution of the model is closer to real output than previous models. The analysis shows that the flow rate is approximately equal in each fracture at the beginning and the gap between fractures is growing in the unsteady stage. The fracture output of the two ends is higher than that of the center because of interference. It is an effective method of increasing production to add the fracture length of the two ends. The distribution of flow rate is wave-like shape due to the influence of fractures with consideration and the flow rate of fractures is symmetric with the well bore. The higher output of the fracture segment that closer to the horizontal well bore, the flux of the middle of the fracture increase as the increase of the heel width and there is an optimized width distribution. The width distribution has significant impact on the fractured horizontal well productivity; according to the established model one can optimize fracture width profile quantitatively.

ACKNOWLEDGEMENTS

We appreciate the work was funded by the following: project (No. 51525404, No. 51504203 and No. 51374178) supported by the National Natural Science Foundation of China, project (No. 2015072) supported by the special fund of China's central government for the development of local colleges and universities, project (No. 2014QHZ004) supported by scientific research starting project of SWPU, project (No.2014PYZ002) supported by scientific research starting project of SWPU and project (szjj2015-020) supported by the open research subject of key laboratory of fluid power machinery and the ministry of education.

REFERENCES

- Al Kobaisi, M., Ozkan, E. & Kazemi, H. 2006. A hybrid numerical/analytical model of a finite conductivity vertical fracture intercepted by a horizontal well. *SPE Reservoir Evaluation & Engineering* 9: 345-355.
- Cinco, L.H. & Samaniego, V.F. 1981. Transient pressure analysis for fractured wells. *Journal of Petroleum Technology* 33: 1749-1766.
- Cinco-L., H., Samaniego-V., F. & Dominguez A., N. 1978. Transient pressure behavior for a well with a finite-conductivity vertical fracture. *Old SPE Journal* 18(4): 253-264.
- Giger, F.M., Reiss, L.H. & Jourdan, A.P. 1984. The reservoir engineering aspects of horizontal drilling. In *SPE Annual Technical Conference and Exhibition*. Texas: Society of Petroleum Engineers.
- Gringarten, A. & Raghavan, R. 1975. Applied pressure analysis for fractured wells. *Journal of Petroleum Technology* 27: 887-892.
- Guo, B. & Schechter, D. 1999. A simple and rigorous IPR equation for vertical and horizontal wells intersecting long fractures. PETSOC-99-07-05. *Journal of Canadian Petroleum Technology* 38(7).
- Joshi S. 1988. Augmentation of well productivity with slant and horizontal wells. *Journal of Petroleum Technology* 40(6): 729-739.
- Joshi, S. 1987. A review of horizontal well and drainhole technology. *SPE Annual Technical Conference and Exhibition*. Texas: Society of Petroleum Engineers.
- Larsen, L. & Hegre, T. 1994. Pressure transient analysis of multifractured horizontal wells. *SPE Annual Technical Conference and Exhibition*, New Orleans, Louisiana, 25-28 September.
- Larsen, L. & Hegre, T. 1991. Pressure-transient behavior of horizontal wells with finite-conductivity vertical fractures. *International Arctic Technology Conference*, Anchorage, Alaska, 29-31 May.
- Li, Z.J., Pu, X.L., Wang, G., Cheng, Y. & Su, Y. 2013. A novel low-fluorescence anti-sloughing agent for a drilling fluid system and its mechanism analysis. *Natural Gas Industry* 33: 97-101.
- Mukherjee, H. & Economides, M. 1991. A parametric comparison of horizontal and vertical well performance. *SPE Formation Evaluation* 6(2): 209-216.

- Prats, M. 1961. Effect of vertical fractures on reservoir behavior-incompressible fluid case. *Society of Petroleum Engineers Journal* 1(2): 105-118.
- Raghavan, R., Cheng, C. & Bijan, A. 1997. An analysis of horizontal wells intercepted by multiple fractures. *SPE Journal* 2(3): 235-245.
- Raghavan, R. & Joshi, S. 1993. Productivity of multiple drainholes or fractured horizontal wells. *SPE Formation Evaluation* 8(1): 11-16.
- Soliman, M.Y., Hunt, J.L. & El Rabaa, A.M. 1990. Fracturing aspects of horizontal wells. *Journal of Petroleum Technology* 42(8): 966-973.
- Sun, H., Yao, J., Lian, P.Q., Fan, D.Y. & Sun, Z.X. 2012. A transient reservoir/wellbore coupling model for fractured horizontal wells with consideration of fluid inflow from base rocks into wellbores. *Acta Petrolei Sinica* 33(1): 117-122.
- van Eekelen, H.A.M. 1982. Hydraulic fracture geometry: Fracture containment in layered formations. *Old SPE Journal* 22(3): 341-349.
- Wang, Z.M., Jin, H. & Wei, J.G. 2009. Interpretation of the coupling model between fracture variable mass flow and reservoir flow for fractured horizontal wells. *Journal of Hydrodynamics* 24: 172-179.
- Wei, Y. & Economides, M.J. 2005. Transverse hydraulic fractures from a horizontal well. *SPE Annual Technical Conference and Exhibition*, Dallas, Texas, 9-12 October.
- Xiao, Y., Wang, T.F., Zhao, J.Z., Hu, Y.Q. & Luo, Y. 2009. Computational model of total stress field while multiple fracturing. *Oil Drilling & Production Technology* 2009(3): 90-93.
- Yuan, Y.Z., Zhang, L.H., Wang, J. & Pu, Y.W. 2009. A binomial deliverability equation for horizontal gas wells in formations with nonlinear seepage flow features. *Oil & Gas Geology* 2009(1): 122-126.
- Zeng, F. & Zhao, G. 2010. The optimal hydraulic fracture geometry under non-Darcy flow effects. *Journal of Petroleum Science and Engineering* 72(1-2): 143-157.

State Key Laboratory of Oil and Gas Geology and Exploration
Southwest Petroleum University
610500, Chengdu
P.R. China

*Corresponding author; email: zengfanhui023024@126.com

Received: 2 July 2015

Accepted: 7 March 2016